VDMA
Fluid Power Association

22nd ISC

International Sealing Conference

Stuttgart, Germany
October 01 - 02, 2024

Sealing Technology –
Challenges accepted!

IMA UNI STUTTGART

ISBN 978-3-8163-0768-6

Fachverband Fluidtechnik im VDMA e. V. Lyoner Str. 18
50628 Frankfurt am Main
Germany

Phone +49 69 6603-1513
E-Mail maximilian.baxmann@vdma.org
Internet www.vdma.org/fluid

Performance of the radial shaft sealing system under the influence of shaft lead

Adrian Heinl, Christian Wilbs, Daniel Frölich

1 Introduction

A tribological system fundamentally consists out of the main components: base body, counter body, intermediate substance, and surrounding medium. The applied load spectrum as well as disturbances form the input variables of the tribological system influence the tribological processes and interactions. Applied to the tribological system of a radial shaft seal (Figure 1) the following system components can be derived:

- Base body → Radial shaft seal
- Counter body → Shaft surface as counter surface
- Intermediate substance → Lubricant to be sealed

The radial shaft sealing system for example is used in gearboxes, wind turbines or robots to seal rotating components. It prevents the leakage of lubricant or the exchange of two media. During use, the operating conditions such as speed, pressure, temperature of the fluid etc. as well as the geometric installation situation influence the system components. The latter and the operating conditions are in constant interaction with each other and determine the performance and lifetime of the radial shaft sealing system. The occurrence of disturbances, such as damage or faulty system components, can lead to unfavorable operating conditions of the system, which in turn can result in poor lubrication, thermal or chemical damage to the components, high wear and ultimately leakage.

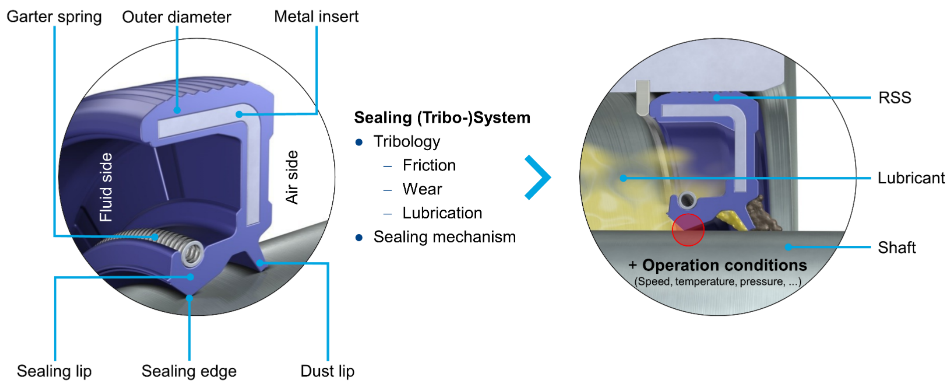

Figure 1: Radial shaft seal (left), complete tribological radial shaft sealing system (right)

In an optimally functioning system, a hydrodynamic fluid film forms between the sealing edge and the shaft surface, i.e. in the sealing gap, under dynamic load. Radial shaft seals (RSS) have a dynamic sealing mechanism that causes the sealed lubricant to be actively pumped in the axial direction, from the air side to the fluid side. This effect is partly responsible for the sealing performance of the radial shaft sealing system. The fluid pumping effect of the sealing system is not only depending on the radial shaft seal but is also significantly influenced by the shaft surface topography. Therefore, the shaft surface roughness parameters must be in an acceptable range. To ensure the performance of the sealing system, in addition to the known roughness parameters, the shaft must be free of fluid pumping structures, so-called shaft lead. Depending on the shaft lead characteristics, lead structures can create an axial pumping effect of the fluid which can lead to either in leakage or poor lubrication conditions and therefore to an increased wear of the sealing system. The effect of shaft lead on the radial shaft sealing system is shown in Figure 2.

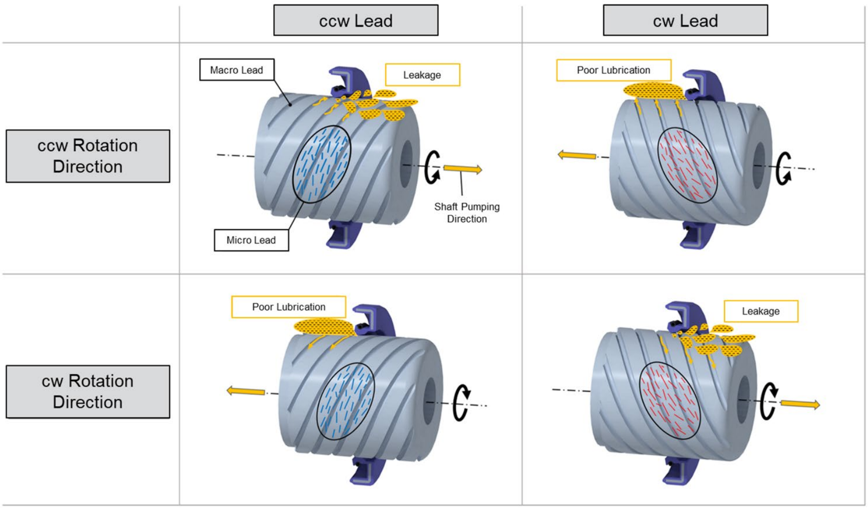

Figure 2: Influence of lead structures on the radial shaft sealing system.

Figure 2 shows how the fluid is pumped in an axial direction depending on orientation of the lead structures and the rotation direction of the shaft, and how this is superimposed on the axial pumping effect of the radial shaft seal, the fluid pumping effect of the radial shaft seal is always from the air side to the fluid side. Regarding to the superimposed fluid pumping effects, two different operating states of the sealing system can be set:

1. The pumping effect of the lead structure is from the fluid side to the air side and thus counteracts the pumping effect of the radial shaft seal. If the shaft pumping effect exceeds that of the radial shaft seal, a net pumping effect towards the air side results, which is expressed in leakage.

2. The pumping effect of the lead structure is from the air side to the fluid side and thus in the same direction as the pumping effect of the radial shaft seal. As a result, the system is subject to poor lubrication, which in turn causes increased wear of the components and increased temperature within the sealing gap.

Both operation conditions can lead to an earlier failure of the sealing system, which in turn can result in significant repair costs and extensive environmental damage.

Due to the variety of manufacturing processes and parameters to produce counter surfaces, shaft lead with different characteristics and scaling can be generated. Shaft lead can be classified into three categories [1], see Figure 3.

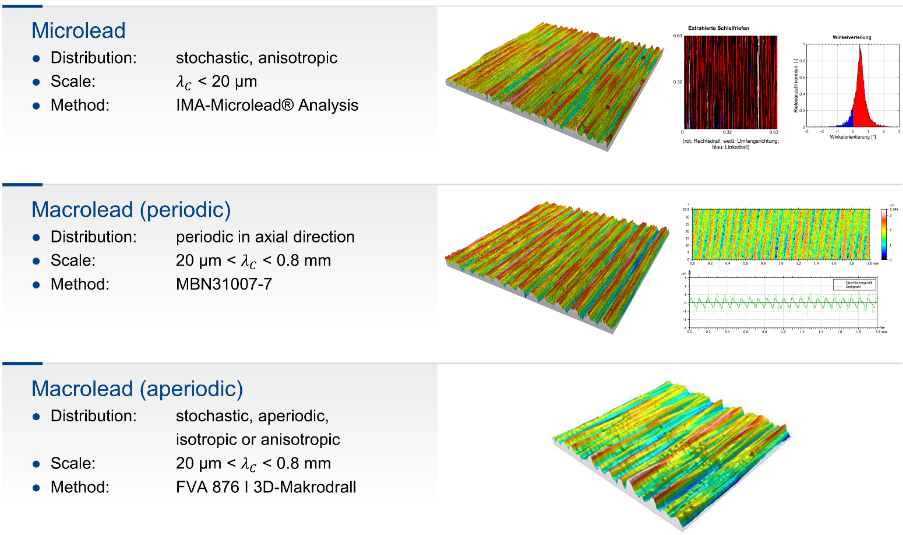

Figure 3: Shaft Lead classification [1]

The longest known characterization method is the CARMEN method according to the Daimler standard MBN31007-7 [2]. This method describes axially and circumferentially periodic lead structures in a scale range of 20 µm to 0.8 mm. The frequency-based analysis method can be used to determine characteristic macrolead parameters such as depth, angle, and period length.

Structures in the same scale range but with an aperiodic and stochastic distribution in axial and circumferential direction, are referred to as aperiodic macrolead or micro waviness [1]. The analysis and evaluation of this shaft lead is not yet available and is part of a research project of the FVA 876 I Research Association for Drive Technology [3].

Individual grooves within the scale range of < 20 µm and are distributed stochastically and anisotropic on the counter surface are referred to as microlead. The IMA-Microlead® Analysis [4] defines the measurement and evaluation of the individual grooves using an optical measurement system and a structure-based algorithm. The algorithm extracts and analysis the geometry characteristics such as angular orientation, length, depth etc. of the grooves.

These different shaft lead categories can be measured and quantified with state-of-the-art measuring and analyzing methods. Using these methods, the correlation between lead parameters and leakage resp. seal wear can be shown. The insights drawn from that analysis, will be applied to unpressurized and pressurized radial shaft sealing systems. Based on the results, limits for an acceptable shaft lead can be set to ensure a reliable sealing system.

2 Measurement methods and test conditions

Chapter 2 describes the used measurement methods and test conditions.

2.1 Shaft lead measurement

To study the performance of the radial shaft sealing system under the influence of shaft lead, plunge ground shafts with different characteristics of microlead and periodic macrolead were examined. The measurement and analysis methods will be explained in more detail in the next chapters.

2.1.1 Microlead measurement acc. IMA-Mikrodrall® Analyse

The microlead measurement uses optical surface measurement instruments to measure the surface topography. The measurement grid consists out of three axial areas and 18 areas in circumferential direction, with a step size of 20 °, around the entire circumference. The measured surface topographies are segmented and the microlead structures are extracted. The corresponding geometric characteristics such as depth, width, length, angle, and volume are then determined for each extracted structure (groove). The determined parameters are evaluated using statistical methods and characteristic distribution curves. The number of all structures and structure volumes with the same angular orientation are added and plotted against the angular orientation. If the median angle of the distribution curve deviates significantly from zero, this means that an increasing number of structures or volumes have an orientation that deviates from the circumferential direction. Figure 4 shows the measurement grid, the geometric groove characteristics, and the distribution curve.

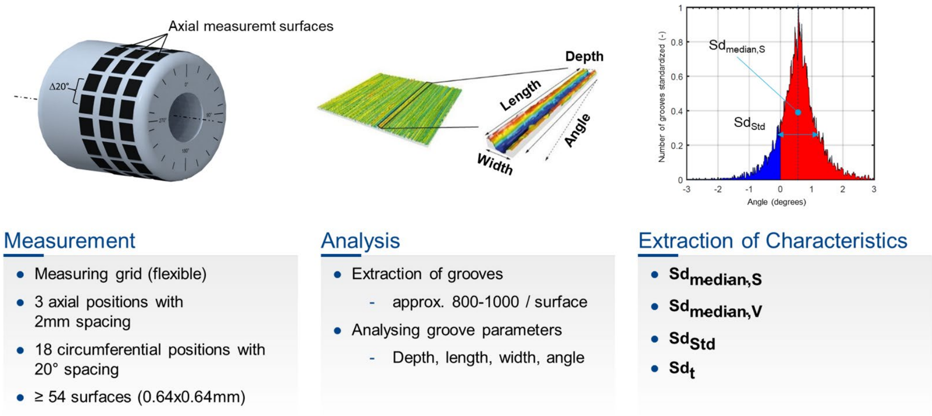

Figure 4: Microlead measurement acc. IMA-Mikrodrall® Analyse [4]

Quantitative microlead parameters can be drawn from the distribution curves by calculating the median angle of the structures $Sd_{\mathrm{median,S}}$ and the median volumes $Sd_{\mathrm{median,V}}$.

2.1.2 Macrolead measurement acc. MBN31007-7

For the analyze of periodic macrolead structures on the counter surface, 72 axial profiles are measured at equal intervals over two measuring grids. Measuring grid 1 extends over a circumferential range of 36 °, with an axial profile spacing of 0.5 °, and measuring grid 2 covers the entire shaft circumference of 360 °, with an axial profile spacing of 5 °. The individual axial profile plots are aligned in the circumferential and axial direction and merge to a 3D pseudo topography. This is followed by a frequency analysis to identify the dominant, periodic macrolead structure. This results in a mathematically approximated lead profile, which is used to determine the macrolead parameters lead depth Dt, lead angle $D\gamma$ and period length DP of the counter surface.

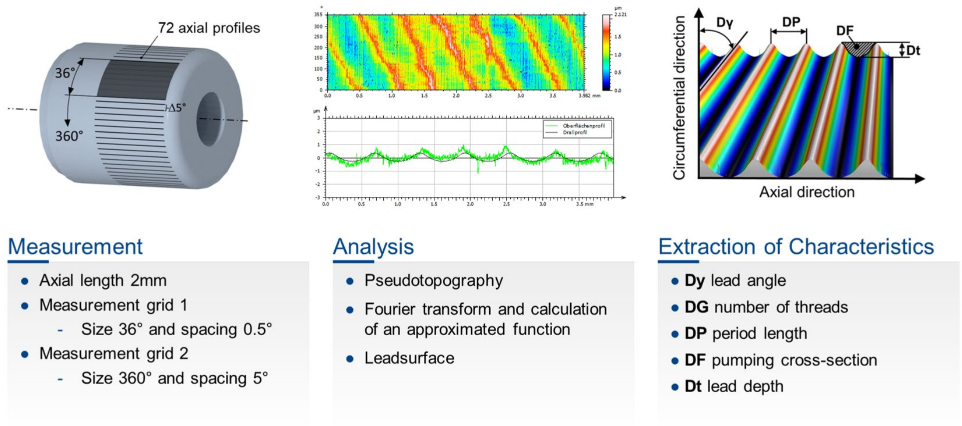

Figure 5: Macrolead measurement acc. MBN31007-7 [2]

2.2 Experimental Test conditions

Certain test conditions were defined and described in the following chapters to measure the shaft pumping rate and to investigate leakage and wear.

2.2.1 Shaft pumping rate measurement

The pumping rate of the sealing system results from the pumping rate of the radial shaft seal and the shaft surface. The pumping rate of the radial shaft seals in usually independent of the shaft rotation direction whereas the pumping rate of the shaft surface can depend on the rotation direction if a shaft lead is present. Depending on the shaft lead orientation and the shaft rotation direction the sealing system pumping rate can be higher or lower compared to a sealing system without shaft lead.

Based on this effect RAAB [5] developed a pumping rate test which make it possible to measure the pumping rate of the counter surface due to shaft lead. The test conditions to carry out the shaft pumping rate measurement are shown in Table 1.

Table 1: Test conditions for shaft pumping rate measurement

Radial Shaft Seal	BAUM3X2, 75 FKM 585
Dimension	35-52-7
Fluid	Mineral gear oil ISO VG 220
Fluid Temperature	80 °C
Shaft sliding speed	5,5 m/s
Test Cycle	1h, 1h, 2h, 2h
Rotation direction	cw, ccw, cw, ccw
Test duration	6 h

2.2.2 Leakage and seal wear tests

The determination of radial shaft sealing system failure due to shaft lead is conducted through a leakage and seal wear tests. Therefore, shafts with and without lead were used. The leakage test was performed by selecting the rotation direction to induce a shaft fluid pumping from the oil to the air side, forcing leakage of the system. The rotation direction for the seal wear tests was selected to induce a fluid pumping from the air to the fluid side, causing poor lubrication conditions and therefore increased wear. Two different sealing system were tested, which are unpressurized, see Table 2, and pressurized, see Table 3.

Table 2: Test conditions for unpressurized sealing system

Investigation	Leakage	Seal wear
Radial Shaft Seal	BAUM3X2	
Dimension	35-52-7	
Material	72 NBR 902 75 FKM 585	
Fluid	Mineral gear oil ISO VG 220	
Fluid Temperature	80 °C	
Shaft sliding speed	5.5 m/s	
Test duration	96 h	504 h
Rotation direction	cw or ccw	

Table 3: Test conditions for pressurized sealing system

Investigation	Leakage	Seal wear
Radial Shaft Seal	BAB, PPS	
Dimension	60-80-7	
Material	75 FKM 595	
Fluid	Hydraulic oil ISO VG 68	
Fluid Temperature	80 °C	
Shaft sliding speed	5.5 m/s	
Pressure	0 bar, 1.5 bar	
Test duration	96 h	240 h
Rotation direction	cw or ccw	

3 Experimental results

The experimental results of the shaft pumping rate measurements as well as the leakage and seal wear tests are shown in the following chapter.

3.1 Results of the shaft pumping rate measurement

In [6] SCHIEFER showed that the influence of periodic macrolead on the fluid pumping rate can be predominantly characterized by the parameters lead depth Dt, lead angle $D\gamma$ and period length DP. The hypothesis which has been formulated is supported by the experimental results of this investigation and state:

1. With an increasing lead depth, the shaft pumping rate increases as well, due to a higher possible pumping volume (Figure 6, A).
2. With an increasing lead angle, the fluid pumping rate increases too, as there are steeper threads for redirecting the fluid below the sealing edge (Figure 6, B).
3. The shaft pumping rate is increasing with decreasing periodic length because there are more lead threads within the sealing contact (Figure 6, C).

The results of the shaft pumping rate measurement are shown in Figure 6. In diagrams the x-axis shows the macrolead parameters and the y-axis the shaft pumping rate PR_{shaft}. Even though, the results show a certain variation the overall trend as described before is obvious.

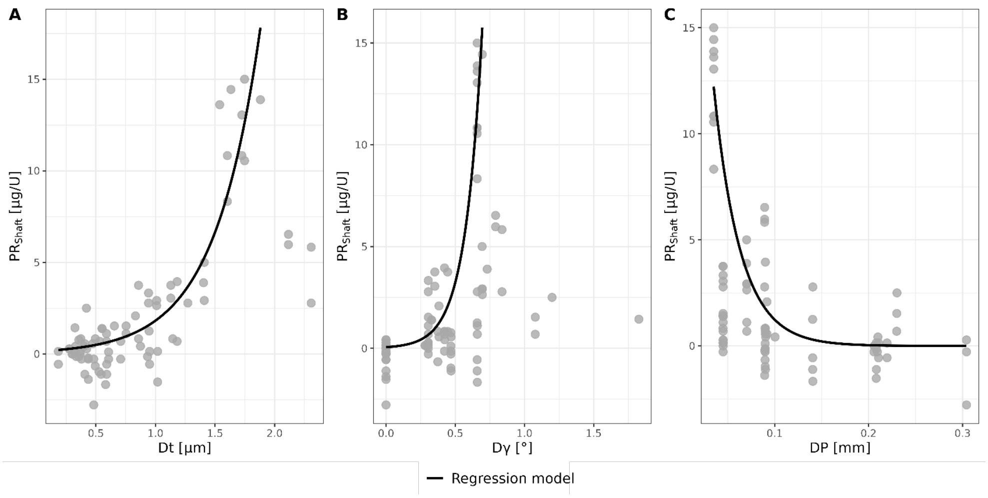

Figure 6: Shaft pumping rate depending on the periodic macrolead parameters

Based on the hypothesis and empirical results, a combination parameter was defined from the three parameters [6]. The combination parameter Km is defined by the following equation:

$$Km = \left|\frac{Dt \cdot D\gamma}{DP}\right| \tag{1}$$

Finally, the shaft pumping rate PR_{shaft} shows a significant linear correlation with the combination parameter Km, see Figure 7.

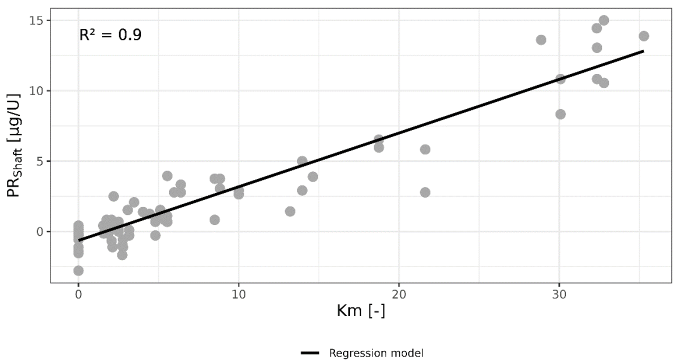

Figure 7: Shaft pumping rate depending on the macrolead combination parameter Km

Microlead shows the same linear correlation as periodic macrolead, but it depends mainly on the microlead parameter $Sd_{\mathrm{median,S}}$, see Figure 8.

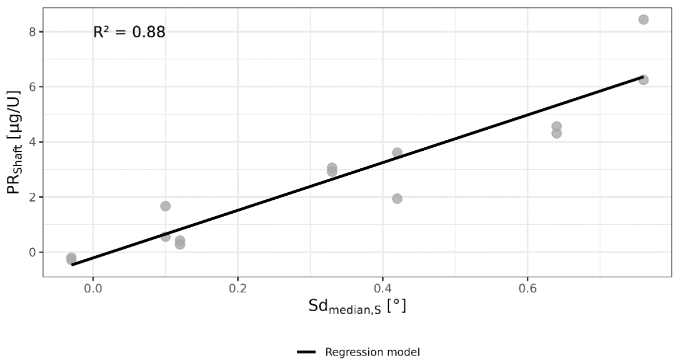

Figure 8: Shaft pumping rate depending on median angle of microlead structures

The shaft pumping rate analysis shows that the lead parameters Km, for periodic macrolead, and $Sd_{\mathrm{median,S}}$, for microlead, provide significant information to characterize and evaluate shaft lead.

3.2 Leakage and seal wear results of the unpressurized sealing system

The following chapter investigates the influence of shaft lead on an unpressurized sealing system. Figure 9 shows the observed leakage rate LR in diagram A and the seal wear band width in diagram B depending on the periodic macrolead characteristics in form of the combination parameter Km. The leakage rate shows an exponential increase with increasing lead characteristic. Concurrently, a noticeable linear increase in the seal wear band width is observed with the increase in macrolead characteristic. The results indicate that periodic macrolead with a Km value greater than 10 affect the analyzed sealing system.

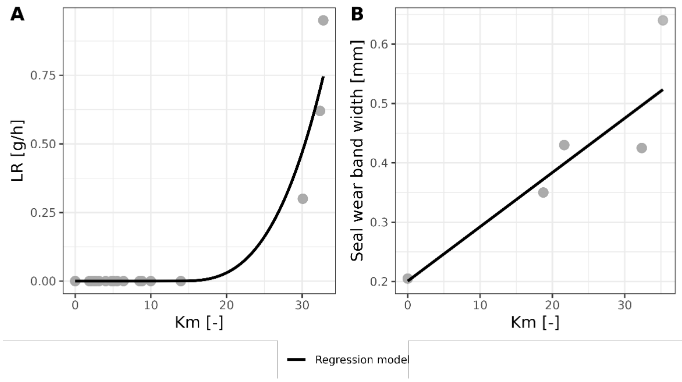

Figure 9: Influence of periodic macrolead structures on unpressurized sealing system

Figure 10 shows the influence of microlead structures on the unpressurized sealing system. Diagram A and B illustrate the relationship between the median angle of the structure distribution $Sd_{\mathrm{median,S}}$ and the leakage rate as well as the seal wear band width. Notably, a median angle of $Sd_{\mathrm{median,S}} > 0.1$ ° results in a significant increase in the seal wear band width. Leakage becomes evident only at a median angle of approximately $Sd_{\mathrm{median,S}} \approx 0.3$ °.

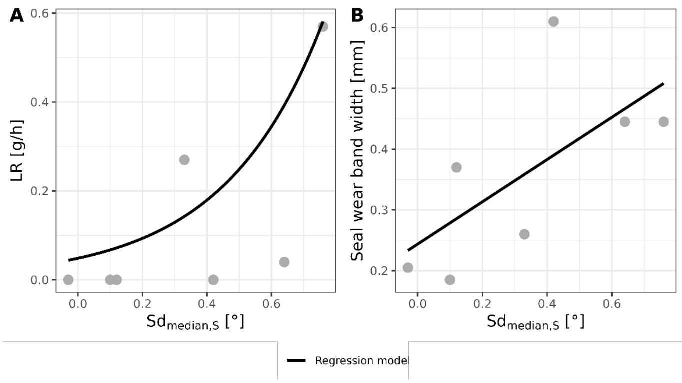

Figure 10: Influence of microlead structures on unpressurized sealing system

3.3 Leakage and seal wear results of the pressurized sealing system

The effects of shaft lead on a pressurized sealing system are shown in the following chapter. Figure 11 shows the correlation between the median angle $Sd_{\mathrm{median,S}}$ and the seal wear as well as the leakage rate of the pressure seals, BAB and PPS, under varying pressure conditions of $0\ bar$ and $1.5\ bar$. The correlation between the median angle (x-axis) and the leakage rate (y-axis) are shown in diagram A. The data indicates that the leakage rate increases exponential with the median angle and elevated pressure levels. Specifically, the unpressurized PPS leaked at a microlead of $Sd_{\mathrm{median,S}} \approx 0.04\ °$. When pressurized, the PPS started leaking at median angle of $Sd_{\mathrm{median,S}} \approx 0.06\ °$. The PPS shows under pressurized operation conditions a higher performance then unpressurized.

Figure 11, diagram A, shows the relationship between the microlead characteristic and seal wear band width. The data show a consistent linear increase in seal wear corresponding to increasing median angles across all tested systems.

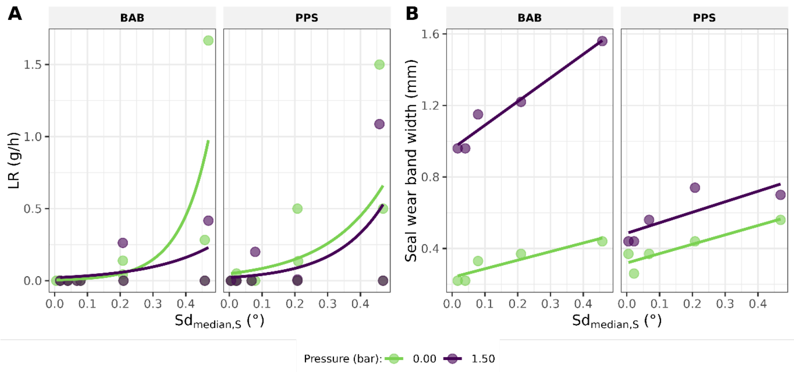

Figure 11: Influence of microlead on a pressurized sealing system

The influence of periodic macrolead on the pressurized sealing system is shown in Figure 12. The leakage test results show slight variations compared to test results with microlead shafts. An increase in the leakage rate with increasing macrolead characteristics is evident for both pressure seals, but this effect is only observable under pressurized conditions. This effect may be attributed to the wider sealing contact induced by pressurize, which increases the number of lead threads within sealing contact and thus can caused a higher fluid pumping of the shaft than that of the seal. The PPS seals leaked at a macrolead characteristic of $Km \approx 2$, whereas the sealing system with the BAB failed at $Km \approx 6$.

Both pressurized and non-pressurized seals show a linear increase in seal wear band width with an increasing macrolead characteristic, shown in diagram B of Figure 12.

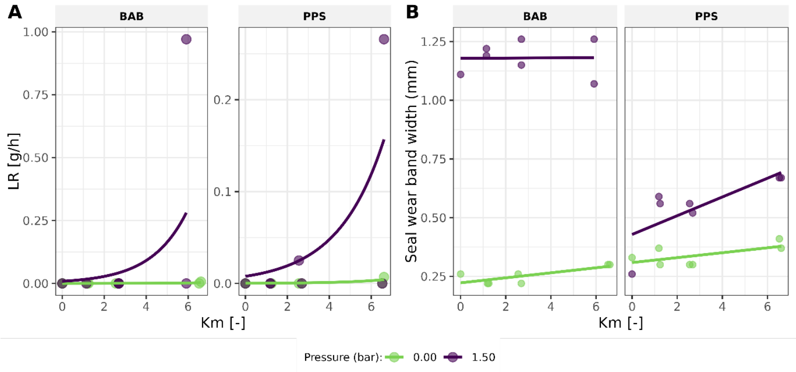

Figure 12: Influence of periodic macrolead on a pressurized sealing system

4 Summary and Conclusion

The performance of a radial shaft sealing system is dependent on the shaft surface. In particular, the sealing system can be disturbed by shaft lead due to the fluid pumping effect. This paper examines the fluid pumping effect of period macrolead as well as microlead, measuring their influence on an unpressurized and pressurized sealing system.

The shaft pumping rate measurement for periodic macrolead indicates that the parameters lead depth Dt, lead angle $D\gamma$ and period length DP significantly influence the shaft pumping effect. This is further corroborated by the combination parameter Km, which shows a significant linear correlation with the shaft pumping rate. Comparable linear relationship was shown by the median angle of microlead structures $Sd_{\mathrm{median},S}$. These results suggest that both macrolead and microlead parameters can be used to predict shaft pumping rates and assess the performance of radial shaft sealing systems.

Additionally, leakage and seal wear tests in both unpressurized and pressurized sealing systems show a consistent increase in leakage rate and seal wear band width as a function of periodic macrolead and microlead. Microlead with a median angular distribution of approximately $Sd_{\mathrm{median},S} \approx 0.04$ ° have been shown to significantly impact on the analyzed radial shaft sealing systems. Regarding to the periodic macrolead, a combination parameter of $Km \approx 2$ has already been shown to be an unsuitable value for a sealing system.

The test results indicates that the influence of the shaft lead depends on the respective radial shaft sealing system with its components and the operating conditions. Further research is needed to determine how variables such as rotation speed, lubricant viscosity or shaft diameter impact the shaft pumping effect thus and, consequently, the overall performance of the sealing system.

5 Nomenclature

Variable	*Description*	*Unit*
λ_c	Gaussian filter	[µm]
Dt	Lead depth	[µm]
DP	Period length	[mm]
$D\gamma$	Lead angle	[°]
DG	Number of threads	[-]
DF	Pumping cross-section	[µm²]
Km	Combination parameter	[-]
$Sd_{\mathrm{median,S}}$	Median angle of the angular structure distribution	[°]
$Sd_{\mathrm{median,v}}$	Median angle of the angular volume distribution	[°]
Sd_{Sdt}	Standard deviation of the angular orientations	[°]
Sd_{t}	Arithmetically averaged structure depths	[µm]
PR_{shaft}	Fluid pumping rate of the shaft	[µg/U]
LR	Leakage rate	[g/h]

6 References

[1] Baumann, M. *Abdichtung drallbehafteter Dichtungsgegenlaufflächen - Messung, Analyse, Bewertung und Grenzen.* Dissertation, Universität Stuttgart: Institut für Maschinenelemente, 2017.

[2] Daimler AG. Teschnische Norm. MBN 31 007-7: *Oberflächenbeschaffenheit. Mess- und Auswerteverfahren zur Bewertung von drallreduzierten dynamischen Dichtflächen.* 2009.

[3] FVA 876 I – 3D-Makrodrall. Research Association for Drive Technology. ger.: Forschungsvereinigung Antriebstechnik e.V.

[4] IMA-Mikrodrall® Analyse. IMA-TechSheet #104140 V1. Universität Stuttgart: Institut für Maschinenelemente.

[5] Raab, H. *Wellenlaufflächen. Einfluss der Wellenlaufflächen auf das Dichtverhalten von Radial-Wellendichtringen.* FKM-Vorhaben. Nr. 211. Universität Stuttgart: Institut für Maschinenelemente. 1998.

[6] Schiefer, F. and Baumann, M. und Bauer, F. *Untersuchung des Förderverhaltens makro-drallbehafteter Dichtungsgegenlaufflächen.* Essen, VDMA Fluidtechnik, 2018. ISBN 978-3-8163-0727.

7 Authors

Freudenberg FST GmbH, Engineering Services

Höhnerweg 2-4, 69469 Weinheim, Germany:

Adrian Heinl, M. Sc., Adrian.Heinl@fst.com

Christian Wilbs, M. Sc., Christian.Wilbs@fst.com

Dr.-Ing. Daniel Frölich, Daniel.Froelich@fst.com

https://doi.org/10.61319/XFODFK5S